

This is a repository copy of Technical and economic performance assessment of blue hydrogen production using new configuration through modelling and simulation.

White Rose Research Online URL for this paper: https://eprints.whiterose.ac.uk/id/eprint/232798/

Version: Published Version

Article:

Li, Y. orcid.org/0009-0006-9771-6559, Ren, J., Ma, H. et al. (1 more author) (2024) Technical and economic performance assessment of blue hydrogen production using new configuration through modelling and simulation. International Journal of Greenhouse Gas Control, 134. 104112. ISSN: 1750-5836

https://doi.org/10.1016/j.ijggc.2024.104112

Reuse

This article is distributed under the terms of the Creative Commons Attribution (CC BY) licence. This licence allows you to distribute, remix, tweak, and build upon the work, even commercially, as long as you credit the authors for the original work. More information and the full terms of the licence here: https://creativecommons.org/licenses/

Takedown

If you consider content in White Rose Research Online to be in breach of UK law, please notify us by emailing eprints@whiterose.ac.uk including the URL of the record and the reason for the withdrawal request.



ELSEVIER

Contents lists available at ScienceDirect

International Journal of Greenhouse Gas Control

journal homepage: www.elsevier.com/locate/ijggc





Technical and economic performance assessment of blue hydrogen production using new configuration through modelling and simulation

Yiming Li^{a,*}, Jiayi Ren^a, Haotian Ma^b, Alasdair N Campbell^a

- ^a Department of Chemical and Biological Engineering, The University of Sheffield, Sheffield S1 3JD, UK
- b Department of Chemical Engineering, The University of Warwick, Warwick CV4 7AL, UK

ARTICLE INFO

Keywords: Technical and economic evaluation Blue hydrogen Steam methane reforming Post-combustion carbon capture Piperazine Energy and cost-saving configuration

ABSTRACT

Steam methane reforming (SMR) is the dominant process for hydrogen production, which produce large amount of carbon dioxide (CO₂) as a by-product. To address concerns about carbon emissions, there is an increasing focus on blue hydrogen to mitigate carbon emissions during hydrogen production. However, the commercialization of blue hydrogen production (BHP) is hindered by the challenges of high cost and energy consumption. This study proposes a new configuration to address these challenges, which is characterized by: (a) the use of piperazine (PZ) as a solvent, which has a high CO₂ absorption efficiency; (b) a more efficient heat exchange configuration which recovers the waste exergy from flue gas; (c) the advanced flash stripper (AFS) was adopted to reduce the capital cost due to its simpler stripper configuration. In addition, the technical and economic performance of the proposed energy and cost-saving blue hydrogen production (ECSB) process is investigated and compared with the standard SMR process. The detailed models of the SMR process and the post-combustion carbon capture (PCC) process were developed and integrated in Aspen plus® V11. The results of the technical analysis showed that the ECSB process with 30 wt.% PZ achieves a 36.3 % reduction in energy penalty when compared to the standard process with 30 wt.% Monoethanolamine (MEA). The results of the economic analysis showed that the lowest levelized cost of blue hydrogen (LCBH) was achieved by the ECSB process with 30 wt.% PZ. Compared to the BHP process with 30 wt.% MEA, the LCBH was reduced by 19.7 %.

1. Introduction

Global hydrogen (H_2) production from fossil fuels was around 90 million tonnes in 2020, which resulted in 900 million tonnes of carbon dioxide (CO_2) emissions (Strategy, 2020). Greenhouse gas emissions are exacerbating global warming. According to the report from the Intergovernmental Panel on Climate Change (IPCC), it is crucial to limit the rise in temperature to 1.5 °C and reach a state of net-zero CO_2 emissions before 2050 (Zhongming et al., 2019). As the global hydrogen demand increases, it is important to consider reducing carbon emissions from hydrogen production.

Currently, around 95 % of hydrogen is produced from fossil fuels, with nearly 50 % of H_2 produced through natural gas reforming (IEA 2021). Steam methane reforming (SMR) is the most widely used technology for hydrogen production. This technology converts methane and steam to H_2 and CO_2 in a fixed-bed reactor with a Ni-based catalyst under high temperature and pressure (Faheem et al., 2021). However, for every tonne of H_2 produced by the SMR process, 7–9 tonnes of CO_2

are released into the atmosphere (Soltani et al., 2014). The hydrogen so produced is often referred to as "grey hydrogen" (Khan et al., 2021). To reduce the greenhouse gas emissions from grey hydrogen, the concept of "blue hydrogen" and "green hydrogen" are increasingly attracting attention.

Blue hydrogen is grey hydrogen combined with carbon capture and storage (CCS). This mitigates the environmental impact as large amounts of $\rm CO_2$ emissions are captured from the SMR unit (Howarth and Jacobson, 2021). Green hydrogen is $\rm H_2$ produce from water electrolysis. The whole process is powered by renewable energy and only produces hydrogen and oxygen (de Fátima Palhares et al., 2018). In the long term, green hydrogen may be the final option for net-zero emissions. However, due to the high cost of green hydrogen, the deployment of blue hydrogen production (BHP) could be an important option in the short term. In a standard BHP plant, $\rm CO_2$ can be captured from 3 different locations: (a) the syngas stream before the $\rm H_2$ separation unit; (b) the tail gas after the $\rm H_2$ separation unit; and (c) the flue gas from the furnace (Collodi et al., 2017). Physical adsorption is often used to capture $\rm CO_2$ from the syngas stream and tail gas, due to the high partial pressure of $\rm CO_2$ here.

E-mail address: yli369@sheffield.ac.uk (Y. Li).

^{*} Corresponding author.

Nomenclature		EPC	Engineering procurement and construction
		GPDC	Generalised pressure drop correlation
a	Order of reaction	HTS	High-temperature water gas shift
C_{i}	Total molar concentration (mol/m³)	IC	Installation cost
E_a	activation energies (kJ/mol)	IEA	International Energy Agency
i	Interest rate	IPCC	Intergovernmental Panel on Climate Change
K	Equilibrium constants	LCBH	Levelized cost of blue hydrogen
k_2	Second-order CO ₂ absorption rate constants (m ³ /kmol s)	LCH	Levelized cost of hydrogen
n	Project life	MEA	Monoethanolamine
P_0	Standard temperature (bar)	O&M	Operating and maintenance
R	Universal gas constant (kJ/kmol K)	OC	Owner's cost
r	reaction rate (m ³ /kmol s)	OPEX	Operational expenditure
T	Temperature (K)	PC	Project contingency
T_0	Standard temperature (°C)	PCC	Post-combustion capture
-		PENG-R	OB Peng Robinson equation of state
Abbrevia		PSA	Pressure swing adsorption
AC	Additional costs	PZ	Piperazine
ACC	Annual capital cost	RK	Redich-Kwong
AFS	Advanced flash stripper	SMR	Steam methane reforming
APEA	Aspen Economic Process Analyzer®	TAC	Total annual costs
BHP	Blue hydrogen production	TEA	Technical and economic analysis
CAPEX	Capital expenditure	TEC	Total equipment cost
CCS	Carbon capture and storage	TIC	Total indirect cost
DEC	Direct equipment cost	TPC	Total plant cost
DFC	Direct field cost	WGS	Water-gas shift
ECSB	Energy and cost-saving blue hydrogen production		
Elec-NR	ΓL Electrolyte Non-Random-Two-Liquid		

Chemical absorption is the most suitable method to capture CO_2 from flue gas since the low pressure of the flue gas. As of 2022, there are three commercial-scale blue hydrogen facilities worldwide, operated by Air Products, Shell and Nutrien (Power et al., 2018; IEA 2018; Terrien et al., 2014). These existing commercial-scale blue hydrogen plants capture CO_2 from the syngas stream with physical adsorption or absorption technologies.

Currently, many studies on BHP investigated the carbon capture from syngas stream and tail gas. Antonini et al. (Antonini et al., 2021) presented an optimized design of a PCC plant using MDEA to capture CO_2 from syngas stream of an SMR plant. Papalas et al. (Papalas et al., 2020) designed a SMR process coupled with Ca-Ni chemical looping to capture CO_2 from syngas. Pellegrini et al. (Pellegrini et al., 2020) investigated a carbon capture process to remove CO_2 from PSA tail gas within an SMR plant. However, a main drawback of these studies are only 35–60 % of the carbon emissions in the whole process can be captured, since the CO_2 from the flue gas is emitted into the atmosphere (Howarth and Jacobson, 2021; Roussanaly et al., 2020). To achieve complete decarbonization of the process, it is important to consider the capture of CO_2 from the flue gas.

Khan et al. (Khan et al., 2021), Roussanaly et al. (Roussanaly et al., 2020), Capocelli et al. (Capocelli et al., 2019) and Subraveti et al. (Subraveti et al., 2021) investigated the carbon capture from flue gas in BHP. However, the high cost of adding the post-combustion carbon capture (PCC) unit hinders the application in BHP. The research of Khan et al. (Khan et al., 2021) showed the increase in the capital cost is estimated \$116.64 million and the increase of operating cost is estimated \$28.3 million/year, when adding a Monoethanolamine (MEA)-based PCC plant to a standalone SMR plant with a capacity of 200 tonne/day of H₂. The studies of Roussanaly et al. (Roussanaly et al., 2020) and Subraveti et al. (Subraveti et al., 2021) showed the CO₂ avoided costs of MEA-based PCC technology used in BHP is around 67–77 \$/t_{CO2}. In addition, more steam is needed to power the carbon capture process, due to the high energy consumption of solvent regeneration. This increase in energy consumption is defined as the energy

penalty. Howarth and Jacobson (Howarth and Jacobson, 2021) pointed out that the high energy penalty is an important challenge of BHP. An additional increase in energy costs of 39 % was estimated when capturing CO_2 from the flue gas.

Currently, the main methods to reduce the energy penalty are applying new solvents and new process configurations (Otitoju et al., 2021). Different solvents have been investigated in the PCC process (Mandal and Bandyopadhyay, 2005; Zhang et al., 2002; Rayer et al., 2012; Rinker et al., 1996; Edali et al., 2009; Derks et al., 2006). The Piperazine (PZ) solvent shows a better energy performance than other solvent, due to its high second-order CO₂ absorption rate constant (k₂) and low activation energy (Ea) (Liang et al., 2015). Compared to MEA, PZ has a higher k2 and a lower Ea value. As a result, the solvent circulation rate of PZ is lower when capturing the same amount of CO2, which means that PZ has lower energy requirements during solvent regeneration process. The experimental studies reported by Van Wagener (Van Wagener et al., 2013), Rochelle and Plaza (Plaza and Rochelle, 2011) showed that the use of PZ instead of MEA can reduce the energy requirements of the PCC process by 10-20 %. Several new configurations have been proposed to reduce energy requirements, such as absorber inter-cooling, stripper inter-heating, exhaust gas recirculation, 2-stage flash configuration and advanced flash stripper (AFS) (Van Wagener et al., 2013; Gao et al., 2019; Diego et al., 2018; Rezazadeh et al., 2017; Li et al., 2016). Amongst them, the use of AFS in the PCC process not only reduces energy consumption, but also achieves a cost reduction of around 22 % (Otitoju et al., 2021).

However, the study of BHP is currently in a fragmented state. Most studies only focus on the hydrogen production or carbon capture process. There is a significant research gap in process design and integration due to the lack of research with a holistic perspective. Several studies on exergy analysis of the SMR process showed the exergy efficiencies is around 62 %-78 % (Dilmac and Ozkan, 2008; Chen et al., 2012; Simpson and Lutz, 2007). The wasted exergy from SMR process is potential to be used in PCC process. In this work, a detailed techno-economic analysis (TEA) of commercial-scale BHP was carried out through modelling and

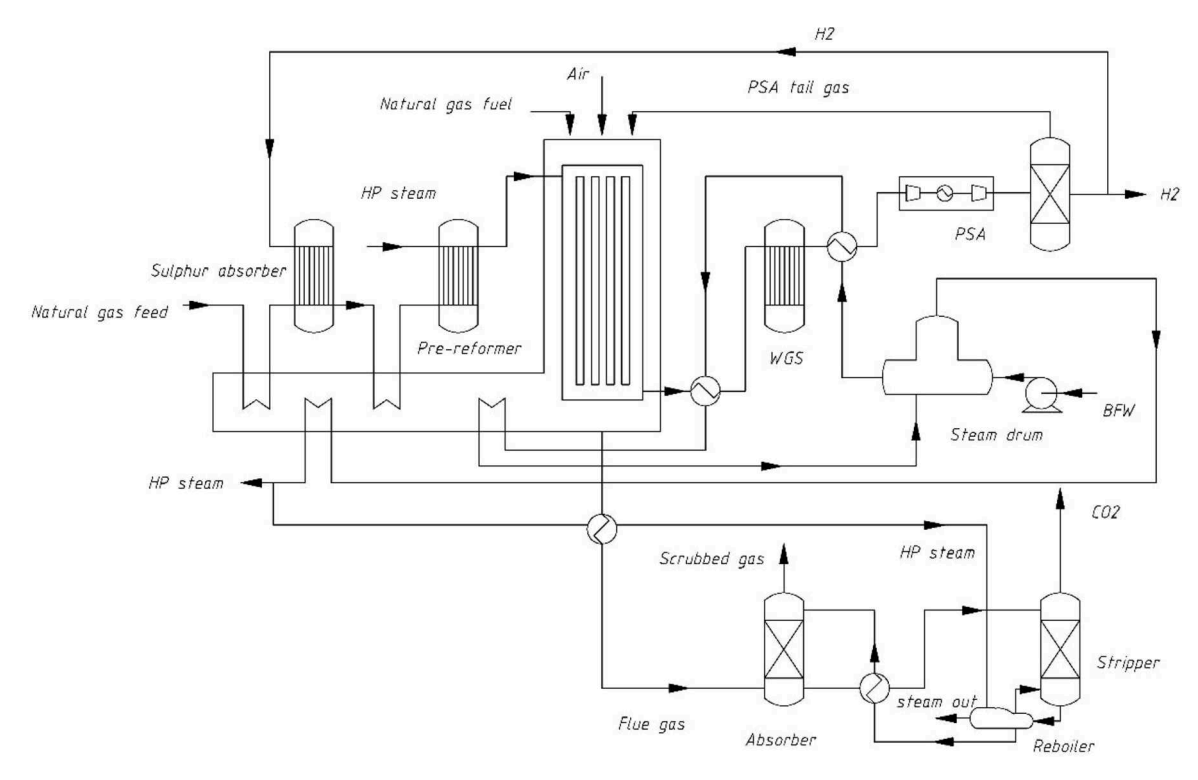


Fig. 1. Diagram of standard BHP process.

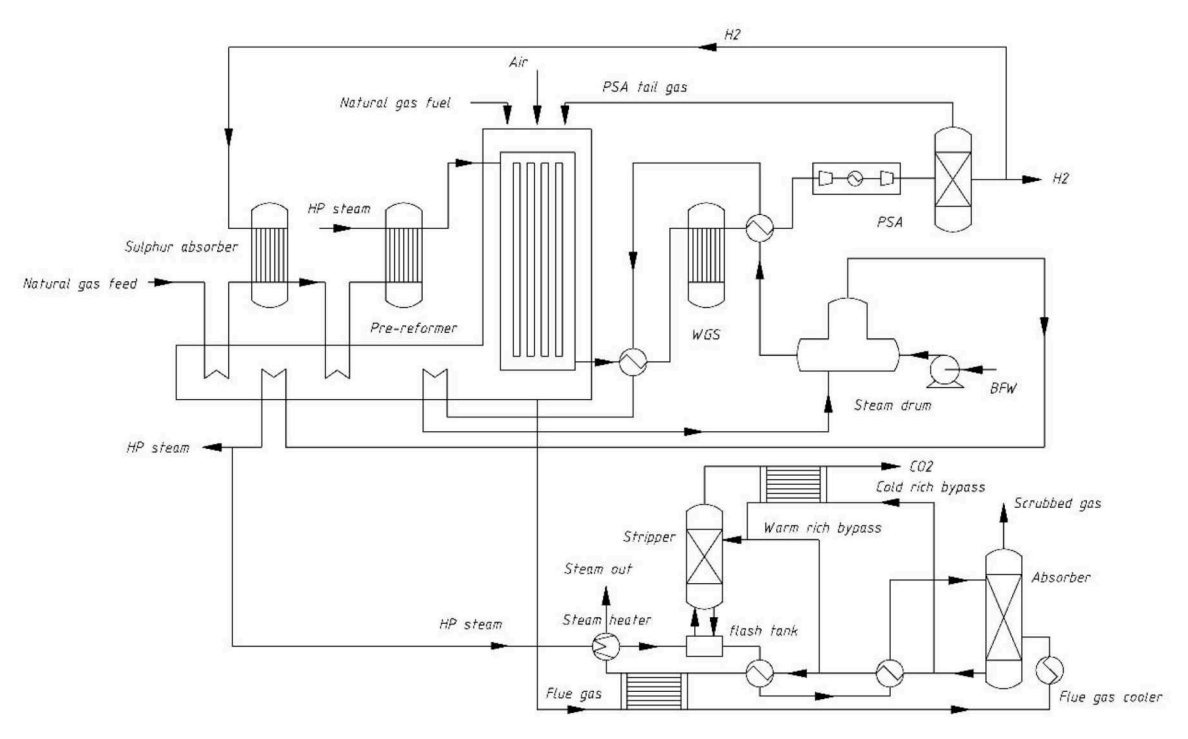


Fig. 2. Diagram of the ECSB process.

simulation. It proposed an energy and cost-saving configuration, which is characterized by: (a) The high absorption efficiency piperazine (PZ) solvent was used to absorb CO_2 ; (b) An energy-saving configuration was designed to recover the waste exergy in the flue gas for heating the solvent regeneration process; (c) The AFS configuration was adopted to reduce the capital cost of the stripper because it does not have a condenser and a reboiler.

2. Methods

2.1. Process description

A standard BHP process is showed in Fig. 1. It consists of a SMR process and a PCC process. Natural gas is pre-heated by flue gas and split as fuel and feedstock. The fuel is combusted in burner to provide the heat for the whole system. The feedstock is blended with recycled H₂ from a

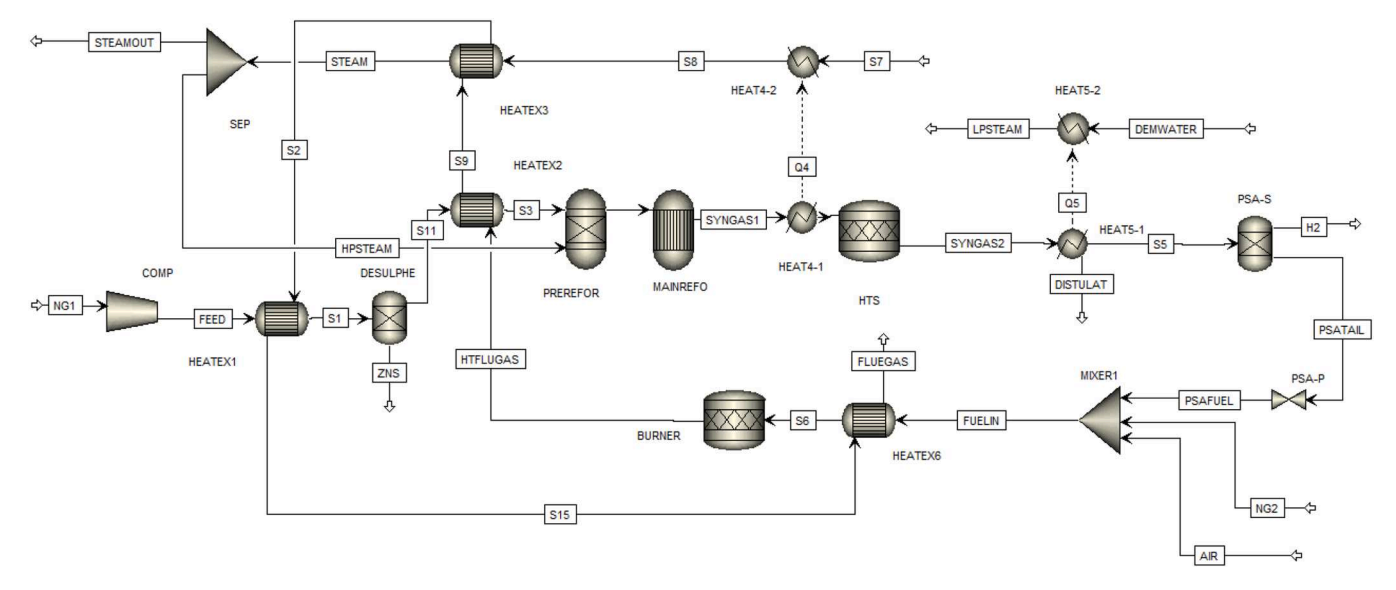


Fig. 3. The flowsheet of the commercial scale SMR plant in Aspen Plus® V11.

pressure swing adsorption (PSA) unit in a desulfurization system, where sulphur components are absorbed in a ZnO bed to prevent catalyst poisoning. The treated feedstock is mixed with high pressure steam in a pre-reformer to convert heavier hydrocarbons (ethane, propane, etc.) to methane. Pre-reformer is a fixed-bed reactor with a Ni-based catalyst, which is responsible for reducing the coking and sintering in the following steps. The product gas from the pre-reformer is then sent to the main reformer to produce syngas at high temperature and pressure. A water gas shift (WGS) reactor is used to convert steam and CO to H2 and CO₂. The shifted syngas is purified in a PSA unit. Around 87 % of the H₂ is separated and the tail gas is sent to the burner as fuel. High pressure steam is generated by recovering the heat from syngas and flue gas. The cooled flue gas is sent to the PCC plant. The CO2 is separated by the CO2lean solvent in the absorber through counter-current contact, yielding the CO₂-rich solvent. The scrubbed gas is then released from top of the absorber. The CO2-rich solvent is heated by the regenerated CO2-lean solvent from the stripper, and then pumped to the stripper. In the stripper, the CO2 is separated from rich solvent at 110 °C-140 °C and discharged from the top of the stripper.

Fig. 2 shows the configuration of the ECSB design. The same configuration of SMR process is adopted while the wasted exergy in the flue gas is recovered to heat the solvent regeneration process. In addition, the AFS was adopted in the PCC process. The rich solvent from the absorber is split into a cold-rich bypass and a warm-rich bypass. The cold-rich bypass is heated by the hot vapour from top of stripper and sent to the top of the stripper after being mixed with part of warm-rich bypass. The rest rich solvent is heated by regenerated lean solvent, flue gas and steam heater before being fed to the flash tank at the bottom of the stripper. The steam heater and the flash tank functioned as the reboiler in the standard stripper.

2.2. SMR system

2.2.1. SMR model development and simulation procedure

A steady-state SMR process was modelled and simulated in Aspen Plus® V11. The Peng Robinson equation of state (PENG-ROB) was used for simulation as it was adopted for non-polar compounds such as CO_2 , CH_4 , H_2 and N_2 . The flowsheet of the SMR plant in Aspen Plus® V11 was shown in Fig. 3.

Natural gas and high pressure steam enters the main reformer after being pressurized and heated. The steam to carbon (S/C) ratio is close to 2.7. Two heater exchange blocks are used to simulate temperature changes of the flue gas and main reformer inlet flow. The main reformer

Table 1
The specifications of main blocks (Collodi et al., 2017).

Block	Main specifications	Value
Main reformer	Temperature (°C)	907
	Pressure (bar)	28
WGS	Temperature (°C)	412
	Pressure (bar)	27.7
Burner	Temperature (°C)	950
	Pressure (bar)	1.034

is simulated as a Gibbs reactor. The main reactions (1) and (2) are equilibrium-limited and highly endothermic.

$$CH_4 + H_2O \leftrightarrow CO + 3H_2, \ \Delta H_{298}^0 = 206 \ kJ/mol$$
 (1)

$$CH_4 + 2H_2O \leftrightarrow CO_2 + 4H_2, \ \Delta H_{298}^0 = 164.9 \ kJ/mol$$
 (2)

The syngas is sent to the WGS reactors after cooling to 320 $^{\circ}$ C. The stoichiometric reactor is used to simulate WGS reactor for correcting the methane conversion rate. The reaction involved is:

$$CO + H_2O \leftrightarrow CO_2 + H_2, \ \Delta H_{298}^0 = -41.1 \ kJ/mol$$
 (3)

In the PSA unit, pure H_2 is separated from the shifted syngas. The PSA tail gas is combusted with natural gas in the burner to provide heat for the system. The burner is simulated as a Gibbs reactor.

The commercial-scale SMR plant is simulated to produce 200 $t_{\rm H2}/$ day. The specifications of main blocks in the model are shown in Table 1.

 $\begin{array}{l} \textbf{Table 2} \\ \textbf{IEA data (Collodi et al., 2017) versus model predictions for SMR plant performance.} \end{array}$

Parameter	IEA data	Model prediction	Relative deviation (%)
CH ₄ conversion rate (%) H ₂ production (kg/h) Flue gas mass flow rate (kg/h) CO ₂ molar concentration in flue gas (%)	84.6 8994 257,698 21.23	86.5 8914 259,584 20.67	2.25 0.89 0.73 2.64
Syngas molar flow rate (kmol/h)	8370.3	8396.2	0.31

Table 3The parameters for the equilibrium and the rate-based reactions.

Equation no.	A	В	С	D
4	132.889	-13,455.9	-22.4773	0
5	216.049	-12,431.7	-35.4819	0
6	-3.03832	-7008.357	0	-0.0031348
8	18.135	3814.4	0	-0.0151
9	14.042	3443.1	0	0

2.2.2. SMR model validation

The commercial-scale SMR process was validated with data from the International Energy Agency (IEA) report (Collodi et al., 2017). This report includes 6 cases of a commercial-scale SMR plant producing 100, $000 \, \text{m}^3$ of H_2 per day without and with CCS. Among them, the Base Case was selected for the validation as it describes the key processes of a standard SMR plant in detail. In this case, the natural gas consumption is around 27 tonne/h, where 85.8 % of the natural gas is used as feedstock the rest is used as fuel. The requirement of high pressure steam in the process is around 86 tonne/h.

The results of the steady-state model validation for methane conversion rate, hydrogen production, flue gas mass flow rate, syngas molar flow rate and CO₂ molar concentration in flue gas are shown in Table 2. The differences between model predictions and IEA data are generally within 5 %. The good agreement shows that the steady-state model satisfactorily predicts the SMR plant performance.

2.3. PCC system

2.3.1. PCC model development

The rate-based models for MEA-based and PZ-based PCC processes were developed in Aspen Plus® V11. The electrolyte Non-Random-Two-Liquid (Elec-NRTL) model was chosen for liquid properties and the Redlich-Kwong (RK) equation of state was used for vapour properties. The chemistry of $\rm CO_2$ absorption with aqueous MEA and PZ is described by both equilibrium and rate-based reactions.

The equilibrium reactions are defined as (Otitoju et al., 2021; Ermatchkov et al., 2006; Canepa et al., 2013)

$$2H_2O \leftrightarrow H_3O^+ + OH^- \tag{4}$$

$$H_2O + HCO_3^- \leftrightarrow H_3O^+ + CO_3^{2-}$$
 (5)

$$H_2O + MEAH^+ \leftrightarrow H_3O^+ + MEA \tag{6}$$

$$H_2O + PZH^+ \leftrightarrow H_3O^+ + PZ \tag{7}$$

$$H_2O + H^+PZCOO^- \leftrightarrow H_3O^+ + PZCOO^- \tag{8}$$

The temperature-dependent equilibrium constants Keq is modelled as

$$In(K_{eq}) = A + \frac{B}{T} + C \cdot In(T) + DT$$
(9)

The rate-based reactions are defined as

$$CO_2 + OH^- \rightarrow HCO_3^- \tag{10}$$

$$HCO_3^- \to CO_2 + OH^- \tag{11}$$

$$MEA + H_2O + CO_2 \rightarrow H_3O^+ + MEACOO^-$$
 (12)

$$H_3O^+ + MEACOO^- \rightarrow MEA + H_2O + CO_2 \tag{13}$$

$$PZ + H_2O + CO_2 \rightarrow H_3O^+ + PZCOO^-$$
 (14)

$$H_3O^+ + PZCOO^- \rightarrow PZ + H_2O + CO_2$$
 (15)

$$PZCOO^{-} + H_2O + CO_2 \rightarrow H_3O^{+} + PZ(COO^{-})_2$$
 (16)

 Table 4

 Kinetic parameter for the rate-controlled reactions.

Equation no.	K	E _a (J/mol)
10	$4.32 e^{+13}$	55,380.82
11	$2.38 e^{+17}$	123,105.18
12	4.77 e ^{+ 11}	41,239.04
13	$2.18\ e^{\ +\ 18}$	59,098.51
14	$7.41 e^{+10}$	33,567.91
15	7.94 e ^{+ 21}	65,837.09
16	$3.62 e^{+10}$	33,567.91
17	$5.56\ e^{\ +\ 25}$	768,226.73

Table 5Relevant correlations for predicting the thermo-physical properties.

Thermo-physical properties	Relevant correlations	Source
Vapour mixture viscosity	Chapman-Enskog-Brokaw model	(Bird et al., 2007)
Viscosity of the liquid mixture	Jones-Dole electrolyte model	(Horvath, 1985)
Vapour phase binary diffusion coefficients	Chapman-Enskog and Wilke-Lee models	(Wilke and Chang, 1955)
Liquid binary coefficient calculations	Wilke-Change model	(Wilke and Chang, 1955)
Thermal conductivity of the vapour mixture	Wassiljewa-Mason-Saxena model	(Plus, 2008)
Thermal conductivity of the liquid mixture	Riedel correlation	(Plus, 2008)
Mixture surface tension	Hakim-Steinberg-Stiel model	(Horvath, 1985)
Mass transfer and interfacial area	Bravo et al. (1985) correlation	(Bravo et al., 1985)
Heat transfer coefficient	Chilton-Colburn analogy	(Chilton and Colburn, 1934)
Liquid holdup	Bravo et al. 1992 correlation	(Bravo et al., 1992)

$$H_3O^+ + PZ(COO^-)_2 \rightarrow PZCOO^- + H_2O + CO_2$$
 (17)

The kinetic expression is defined as

$$r = KT^n \exp\left(-\frac{E_a}{RT}\right) \prod_{i=1}^{N} C_i^{a_{ij}}$$
(18)

The values of the parameter for the equilibrium and the rate-based reactions are given in Tables 3 and 4 (Canepa et al., 2013; Posey and Rochelle, 1997; Hetzer et al., 1968; Ermatchkov et al., 2003; Pinsent et al., 1956; Bishnoi and Rochelle, 2000).

Relevant correlations for predicting the thermophysical properties of the liquid and vapour phases were shown in Table 5.

2.3.2. PCC model validation

The MEA-based and PZ-based PCC models were validated by comparison with pilot scale measurements. The MEA-based PCC model was validated with the experiment data from the Tarong PCC pilot plant in

Table 6The main specifications of the MEA-based and PZ-based PCC pilot plant (Plaza and Rochelle, 2011; Li et al., 2016; Van Wagener, 2011).

	Main specifications	value
MEA-based PCC plant	Condenser temperature (°C)	17
	L/G ratio (mol/mol)	3.27
	Solvent circulation rate (kg/h)	1636.2
	Stripper top pressure (bar)	2
	Lean loading (mol _{CO2} /mol _{MEA})	0.283
PZ-based PCC plant	Condenser temperature (°C)	14.9
_	L/G ratio	5.5
	Solvent circulation rate (kg/h)	3744
	Stripper top pressure (bar)	1.38
	Lean loading (mol _{CO2} /mol _{PZ})	0.285

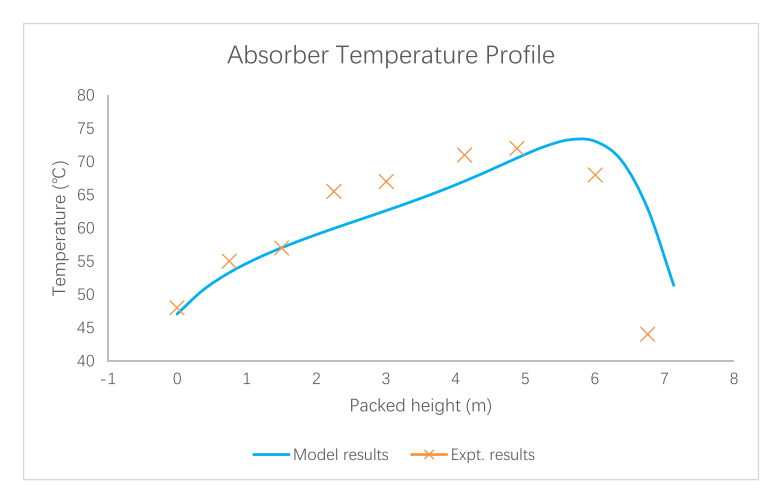


Fig. 4. Model validation for absorber temperature profile of MEA-based PCC model.

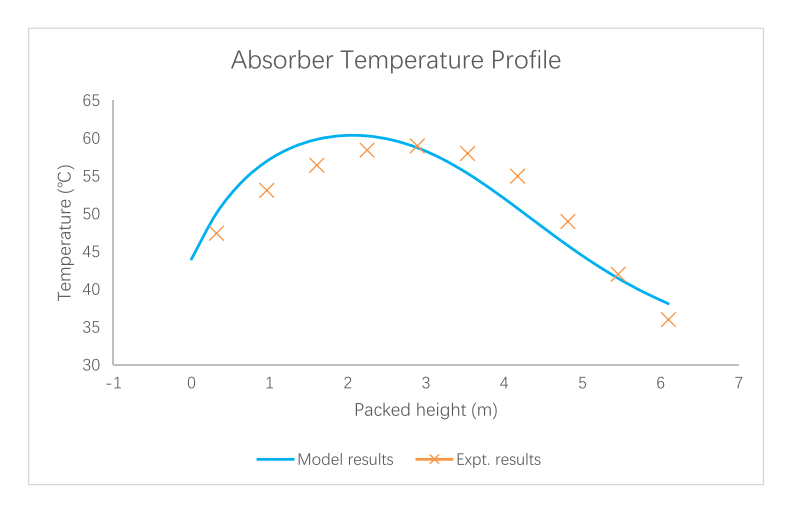


Fig. 5. Model validation for absorber temperature profile of PZ-based PCC model.

Table 7Model validation for MEA-based PCC plant performance.

Parameter	Experiment	Simulation	Relative deviation (%)
Rich loading (mol _{CO2} / mol _{Alk})	0.492	0.486	1.42
CO ₂ removal (%)	84.45	80.04	5.22
CO ₂ product purity (vol%)	99.5	99.6	0.1
Reboiler duty (MJ/kg CO ₂)	4.11	4.25	3.41

Queensland, Australia (Li et al., 2016). The MEA solvent with a concentration range of 24–34 wt.%, was used in the test of 22 cases. The flue gas contained 11.1–13.5 vol% carbon dioxide. The absorber had a diameter of 0.35 m and consisted of four 1.784 m sections packed with Mellapak M250X. The stripper had a diameter of 0.25 m and consisted of two 3.584 m sections packed with Mellapak M350X.

The PZ-based PCC model was validated against experimental data from University of Texas at Austin (Plaza and Rochelle, 2011; Van Wagener, 2011). The PZ solvent, with a concentration range of 28–44 wt.%, was used in the test of 14 cases. The flue gas contained 12 vol% CO₂. The absorber and stripper had a diameter of 0.427 m and consisted of two 3.05 m sections packed with Mellapak 2 X. The key operating parameters of the MEA-based and PZ-based PCC pilot plant are included in Table 6.

The results of MEA-based and PZ-based PCC model predictions

 $\begin{tabular}{ll} \textbf{Table 8} \\ \textbf{Model validation for PZ-based PCC plant performance.} \\ \end{tabular}$

Parameter	Experiment	Simulation	Relative deviation (%)
Rich loading (mol _{CO2} / mol _{Alk})	0.384	0.383	0.26
CO ₂ removal (%)	85.9	81.2	5.47
CO ₂ rate (kg/s)	0.033	0.034	3.03
Rich flowrate (kg/s)	1.10	1.10	0
Reboiler duty (MJ/kg CO ₂)	130.6	127.0	2.76

against experimental data for absorber temperature profile are shown in Figs. 4 and 5. The MEA-based and PZ-based PCC model validation results of rich loading, capture level, reboiler temperature and heat duty are shown in Tables 7 and 8. It can be concluded that the MEA-based and PZ-based PCC models satisfactorily predicted the experimental results as deviations are within ± 10 %.

2.3.3. Model scale-up

The MEA-based and PZ-based PCC models were scaled up to capture 90% of CO_2 from the commercial-scale SMR plant. The mass flow rate of the flue gas from the SMR plant are 72.1 kg/s, which consists of N_2 (61 mol%), CO_2 (20.7 mol%), H_2O (17.5 mol%), O_2 (0.8 mol%). The solvent circulation rate was estimated by the approach proposed by Agbonghae et al. (Agbonghae et al., 2014). It calculated the solvent circulation rate

Table 9Dimensions of columns for commercial-scale PCC plant.

	Parameters	Value
MEA-based PCC plant	Absorber column diameter (m)	8.9
	Absorber packing height (m)	10
	Absorber packing type	Mellapak M250X
	Stripper column diameter (m)	7.2
	Stripper packing height (m)	10
	Stripper packing type	Mellapak M350X
PZ-based PCC plant	Absorber column diameter (m)	7.8
•	Absorber packing height (m)	10
	Absorber packing type	Mellapak 2X
	Stripper column diameter (m)	6.5
	Stripper packing height (m)	10
	Stripper packing type	Mellapak 2X

Table 10The performance of MEA-based and PZ-based PCC plant at commercial scale.

	Parameters	Value
MEA-based PCC plant	Solvent circulation rate (kg/s)	516
	Lean loading (mol _{CO2} /mol _{MEA})	0.283
	Capture level (%)	90
	MEA concentration (wt.%)	30 %
	Absorber pressure (bar)	1.1
	Stripper pressure (bar)	2.4
PZ-based PCC plant	Solvent circulation rate (kg/s)	250-475
	Lean loading (mol _{CO2} /mol _{PZ})	0.287
	Capture level (%)	90
	PZ concentration (wt.%)	30-44
	Absorber pressure (bar)	1.1
	Stripper pressure (bar)	1.8

based on the solvent absorption capacity that obtained from pilot plant. The diameter of columns was calculated by the generalised pressure drop correlation (GPDC) method (Sinnott, 2005). This method first calculates the flow parameters which is the ratio of the liquid to gas entering the packed column. Then, a modified gas load can be obtained from the generalised pressure drop correlation. Finally, the column diameter can be calculated based on the gas mass flow rate per unit cross-sectional area. Other parameters were obtained from pilot plant simulation. The values of the column diameter and height used to simulate the commercial-scale PCC process are shown in Table 9. The simulation of MEA-based and PZ-based PCC process at commercial scale were carried out in Aspen Plus® V11. The performance of commercial-scale PCC processes is shown in Table 10 and the flowsheet

of a commercial-scale solvent-based PCC plant is shown in Fig. 6.

2.4. Process integration and energy and cost-saving configuration design

The standard configuration of commercial-scale SMR process integrated with PCC process was developed in Aspen Plus® V11. The flowsheet of the standard configuration is shown in Fig. 7. In the standard configuration, the flue gas is usually cooled down to 40-50 °C before entering the PCC process, since high temperature will increase the solvent losses by evaporation. The flue gas cooling system is modelled as a heater block (GASCOOLE). To reduce the energy penalty of solvent regeneration in the PCC process, the energy and cost-saving configuration was designed. The wasted exergy from the flue gas stream in the SMR process was used to heat the rest rich solvent in the PCC process by a heat exchanger which represented by two heater blocks (HEAT9-1 and HEAT9-2) connected by a heat stream (QEX). The AFS configuration was adopted to reduce the capital cost of the stripper because it does not have a condenser and a reboiler. The flowsheet of energy and cost-saving configuration developed in Aspen Plus® V11 was shown in Fig. 8.

2.5. Technical and economic evaluation

2.5.1. Energy performance evaluation

The energy performance of different solvents in a standalone PCC plant was evaluated at first. The duty of heat for reboiler, cooling for condenser and electricity for pumps was unified into the ratio representing the energy required in gigajoules (GJ) per tonne of CO_2 . This presents the energy consumption on a similar basis and helps in determine the best solvent selection.

Then, the energy performance of commercial-scale BHP using different solvents and configurations was investigated. The SMR process without carbon capture was evaluated as a benchmark. The energy consumption of different units in BHP was unified to equivalent work. The increase of total energy consumption was defined as the energy penalty, which was calculated by Eq. (19):

$$Energy penalty = \left(\frac{Energy demand with PCC - Energy demand without PCC}{Energy demand without PCC}\right)$$

$$*100$$

$$(19)$$

2.5.2. Economic performance evaluation

The economic analysis of the BHP was performed using the Aspen

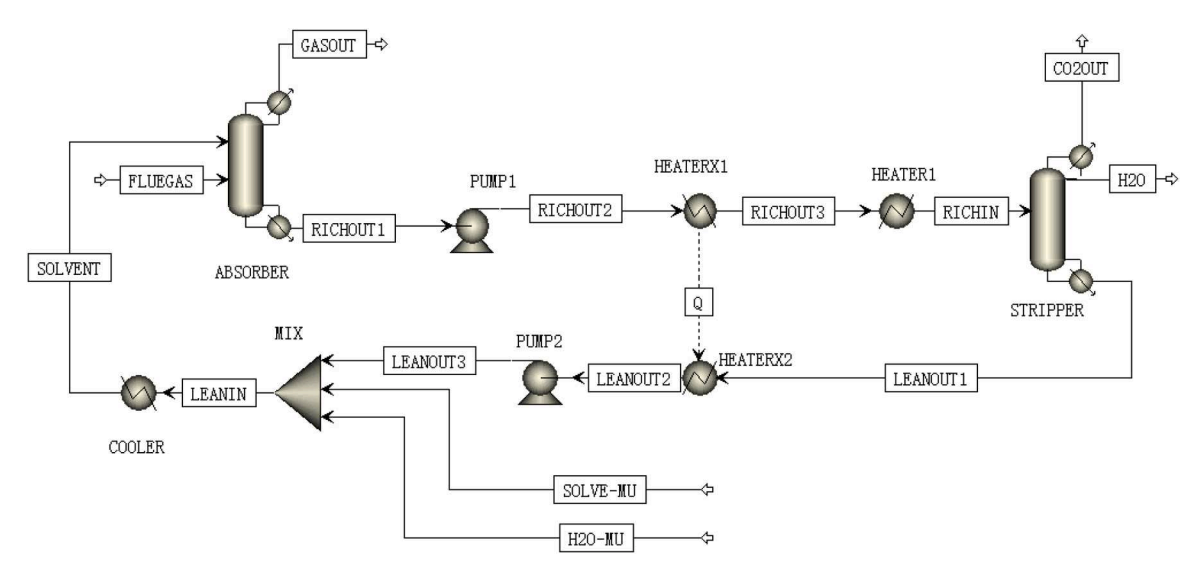


Fig. 6. The flowsheet of commercial-scale solvent-based PCC plant in Aspen Plus® V11.

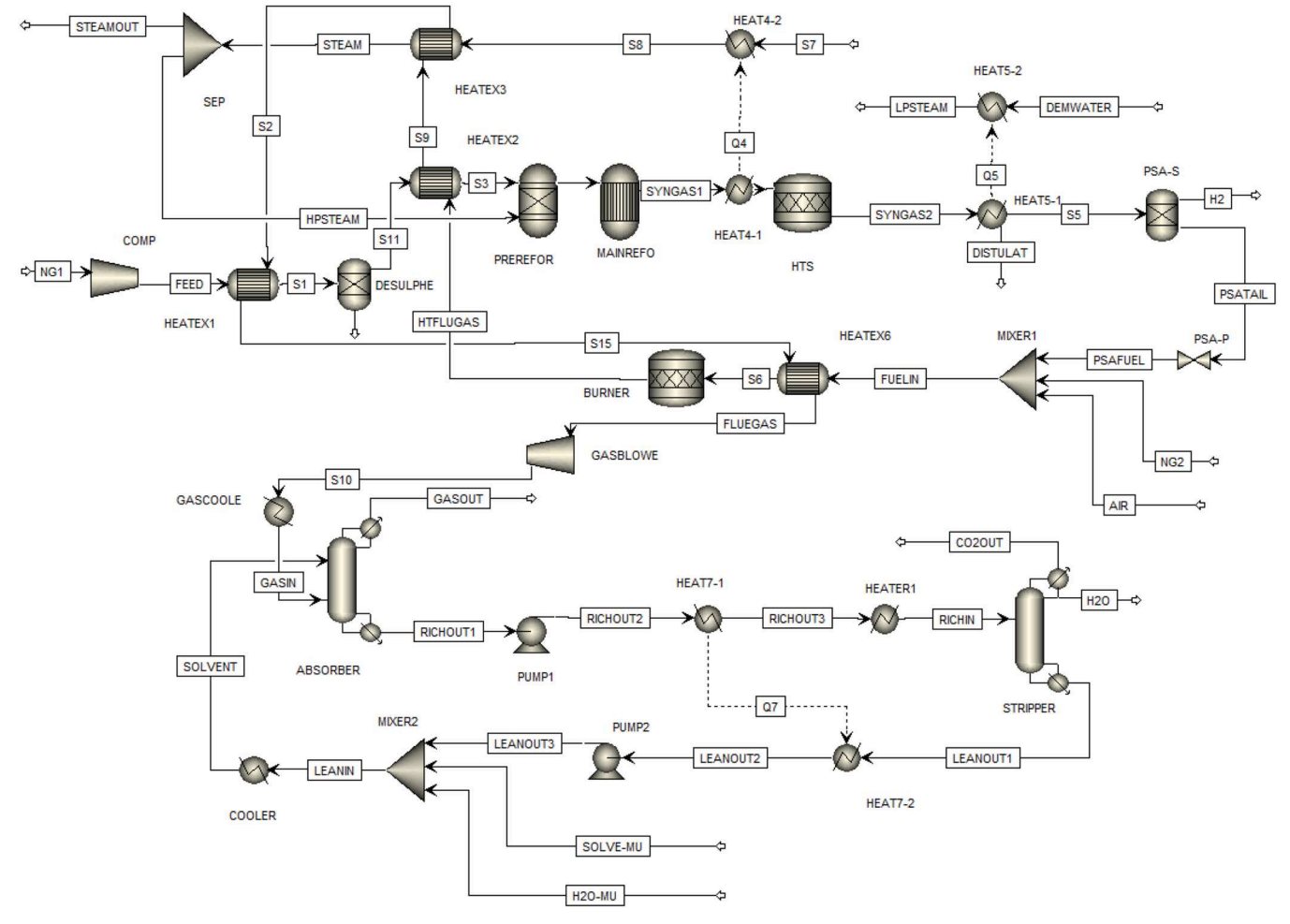


Fig. 7. The flowsheet of standard BHP in Aspen Plus® V11.

Economic Process Analyzer® (APEA) based on the detailed process flowsheet shown in Figs. 6 and 7. The developed models were exported to APEA and then each unit was sized and calculated according to relevant design codes. APEA calculates the direct costs of BHP process equipment such as the fixed-bed reactors, furnace, PSA, heat exchangers, compressors, pumps, and columns. The process stream pipes and splitters are not represented as project components. The capital expenditure (CAPEX) is calculated with the direct equipment cost (DEC). The operational expenditure (OPEX) includes fixed annual operating and maintenance (O&M) costs and variable O&M costs. The fixed O&M costs were assumed as 3 % of the CAPEX (Luo, 2016), which includes operating labour costs, maintenance cost, overhead charges etc. The variable O&M costs include natural gas, steam, solvent consumption, and utility costs. The solvent loss value of 1.5 kg/ t_{CO2} was chosen for MEA (Otitoju et al., 2021; Lepaumier et al., 2011) and 0.05 kg/t_{CO2} was chosen for PZ (Manzolini et al., 2015). The prices of the consumables and utilities are shown in Table 11.

The total annual costs (TAC) include annual capital costs (ACC) and annual O&M costs. The ACC was calculated by Eq. (20) (Karimi et al., 2011),where n is the project life and i is the interest rate. Based on the general project lifetime and interest rate in hydrogen production, n=25 and i=10% are assumed to ensure that the analysis accurately reflected the costs and benefits (Collodi et al., 2017).

$$ACC = \frac{CAPEX}{[(1+i)^n - 1]/i(1+i)^n}$$
 (20)

3. Results and discussion

3.1. Energy performance results

Table 12 shows the contributions of heat duty, cooling duty and electric duty to the energy performance of different solvents. The values of duty were normalized by the tonnes of CO_2 captured. The heat duty is contributed by reboiler while the electric duty is contributed by pumps. The 30 wt.% MEA has the highest heat duty of 4.286 GJ/ t_{CO2} and electric duty of 7.255 MJ/ t_{CO2} . Comparing to the PCC process using 30, 38 and 44 wt.% PZ, the PCC process using 30 wt.% MEA has a higher energy penalty on solvent regeneration. In addition, when the lean loading of PZ is low, the energy consumption of carbon capture increases with the increase of PZ concentration. This result was also observed in the research by Gaspar et al. (Gaspar et al., 2016).

The cooling energy consumption is comprised of the flue gas cooling duty (from GASCOOLE), regenerated solvent cooling duty (from COOLER) and condenser duty of the stripper (from STRIPPER). The highest cooling duty of 4.72 GJ/t_{CO2} achieved by the PCC process using 30 wt.% MEA. The PCC process using PZ achieved 8 %, 19 % and 29 % reduction in cooling duty when the PZ concentration increase from 30 to 44 wt.%. The regenerated solvent cooling (COOLER) is the main factor leading to the change of cooling duty. The reduction of solvent circulation rate results in the reduction of regenerated solvent cooling duty, which leads to the cooling duty to decrease.

Fig. 9 shows the energy performance of commercial-scale BHP using different solvents and configurations. It is evident that alterations in both solvent and configuration result in variations in the total energy

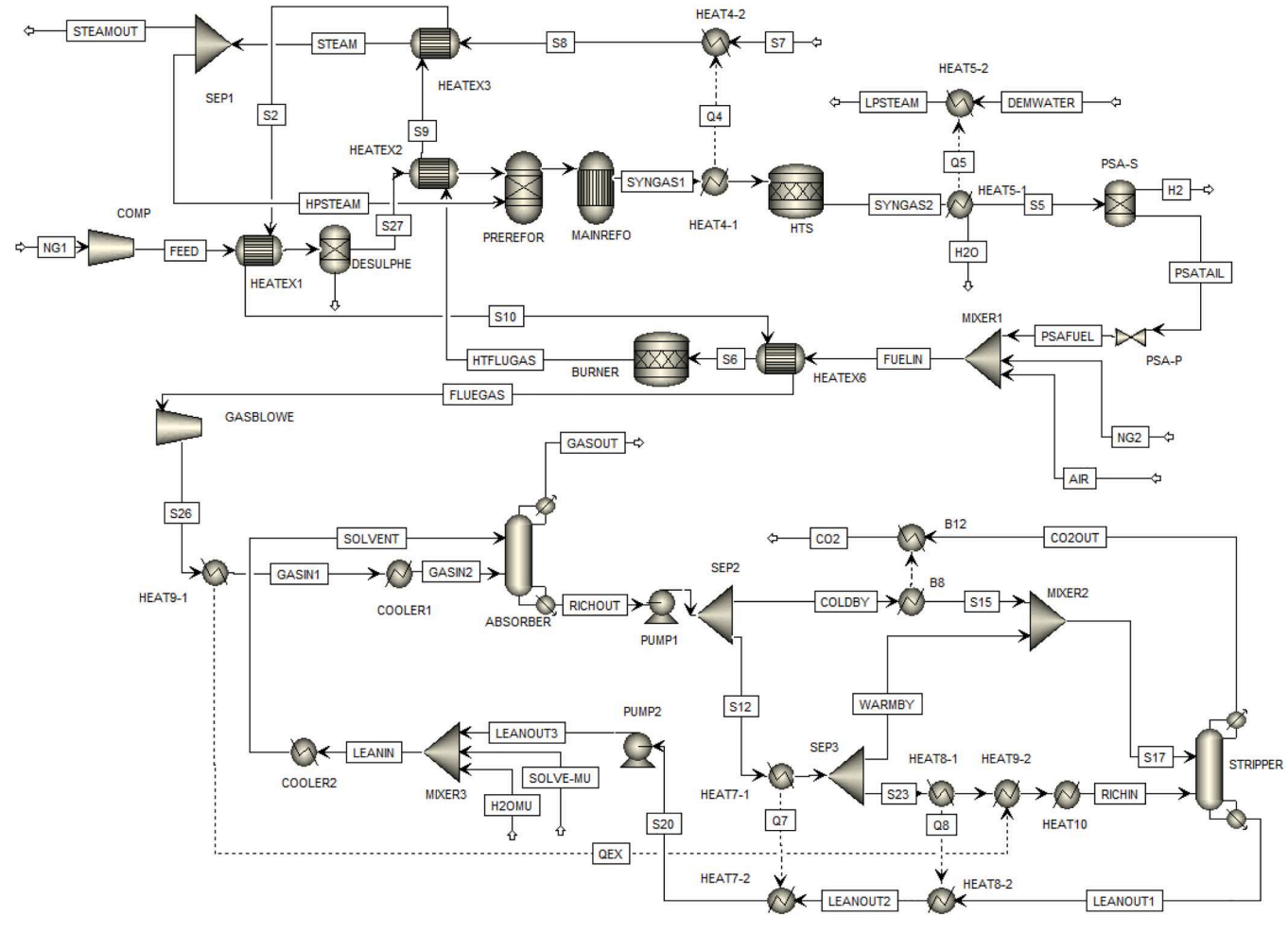


Fig. 8. The flowsheet of ECSB in Aspen Plus® V11.

Table 11
The reference prices of consumables and utilities in February 2023 (IEA 2021; Otitoju et al., 2021; TRADING ECONOMICS 2023).

Item	value
Natural gas price (\$/mmbtu)	3.64
Electricity price (\$/kW)	0.406
Make-up water cost (\$/tonne)	3
Make-up MEA cost (\$/tonne)	1500
Make-up PZ cost (\$/tonne)	8000

Table 12The energy performance of PCC with different solvents.

Concentrations	Heat duty (GJ/t _{CO2})	Cooling duty (GJ/t _{CO2})	Electric duty (MJ/t _{CO2})	Total duty (GJ/ t _{CO2})
30 wt.% MEA	4.286	4.720	7.255	9.013
30 wt.% PZ	3.280	4.341	3.363	7.625
38 wt.% PZ	3.885	3.778	3.378	7.668
44 wt.% PZ	4.276	3.348	1.707	7.625

consumption of BHP. Their contributions to the change in total energy consumption are nearly equal. The use of PZ solvent and ECSB configuration significantly reduces the energy penalty associated with the PCC process but has little impact on the SMR process. Among them, the use of

30 wt.% PZ achieved the largest reduction in energy penalty. This finding is consistent with the performance of different solvents in a standalone PCC plant.

The detailed energy required to operate each of the units is listed in Table 13. The total energy consumption of the SMR process without carbon capture is 154.61 MW of which 95.9% is used for the heating the reactors. The integration of the PCC process slightly increases the energy demand of the SMR process, primarily reflected in the increase of energy consumption by the air blower. This stems from the fact that all the energy required by the PCC process is provided by the furnace in the SMR process. Therefore, additional natural gas is burned to produce more steam, which is used to power the solvent regeneration process. This leads to an increase in flue gas flowrate. Thus, more energy was required by air blower for sending more flue gas into the absorber. Among the use of different solvents and configurations, the highest energy penalty of 59.32% is obtained in the BHP with 30 wt.% MEA, which is mainly caused by the high energy demand for solvent regeneration. The use of 30 wt.% PZ significantly reduces the energy penalty caused by solvent regeneration. The new configuration further reduces the energy penalty caused by the carbon capture process. The lowest total energy consumption of BHP process is achieved by ECSB with 30 wt.% PZ. Compared with BHP with 30 wt.% MEA, the energy penalty is reduced by 36.35 %.

3.2. Economic evaluation results

The DEC obtained from the APEA is shown in Table 14. The SMR process without carbon capture was evaluated as a baseline. The

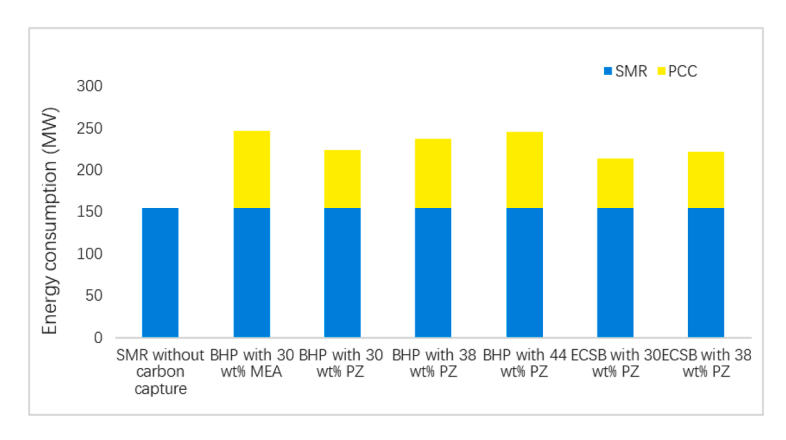


Fig. 9. Energy performance of commercial-scale BHP using different solvents and configurations.

Table 13Detailed energy required to operate each of the units in BHP.

	SMR without carbon capture	BHP with 30 wt.% MEA	BHP with 30 wt.% PZ	BHP with 38 wt.% PZ	BHP with 44 wt.% PZ	ECSB with 30 wt.% PZ	ECSB with 38 wt.% PZ
Hydrogen production							
Natural gas compressor (MW)	4.93	4.93	4.93	4.93	4.93	4.93	4.93
Reactors heating (MW)	148.34	148.34	148.34	148.34	148.34	148.34	148.34
Air blower (MW)	1.34	1.49	1.46	1.48	1.49	1.44	1.45
Carbon capture							
Flue gas blower (MW)	N/A	2.09	2.03	2.07	2.09	2.01	2.03
Solvent pump (MW)	N/A	0.18	0.077	0.072	0.039	0.055	0.052
Solvent regeneration (MW)	N/A	89.30	66.50	80.50	88.60	56.22	64.99
Total energy consumption (MW)	154.61	246.33	223.33	237.39	245.49	212.99	221.79
Energy penalty (%)	N/A	59.32	44.45	53.54	58.78	37.76	43.45

Table 14
The DEC of commercial-scale BHP process with different configurations.

	SMR without carbon capture	BHP with 30 wt.% MEA	BHP with 30 wt.% PZ	BHP with 38 wt.% PZ	BHP with 44 wt.% PZ	ECSB with 30 wt.% PZ	ECSB with 38 wt.% PZ
Reactors (Million \$)	5.05	5.05	5.05	5.05	5.05	5.05	5.05
PSA (Million \$)	0.22	0.22	0.22	0.22	0.22	0.22	0.22
Furnace (Million \$)	23.74	28.62	27.38	28.14	28.54	26.82	27.29
Heat exchangers (Million \$)	0.38	4.44	3.48	2.80	1.47	1.83	1.75
Coolers (Million \$)	0.40	1.70	1.09	1.05	1.05	0.96	1.05
Compressors (Million \$)	14.52	17.50	16.74	17.21	17.46	16.40	16.69
Pumps (Million \$)	N/A	0.76	0.48	0.45	0.27	0.47	0.44
Columns (Million \$)	N/A	12.55	8.99	11.36	14.10	7.31	7.42
DEC (Million \$)	44.30	70.82	63.42	66.27	68.15	59.04	59.92

Table 15
The CAPEX of commercial-scale BHP process with different configurations.

	SMR without carbon capture (Million \$)	BHP with 30 wt.% MEA (Million \$)	BHP with 30 wt.% PZ (Million \$)	BHP with 38 wt.% PZ (Million \$)	BHP with 44 wt.% PZ (Million \$)	ECSB with 30 wt.% PZ (Million \$)	ECSB with 38 wt.% PZ (Million \$)
DEC	44.30	70.82	63.42	66.27	68.15	59.04	59.92
Total indirect cost (TIC)	8.86	14.16	12.68	13.25	13.63	11.81	11.98
Direct field cost (DFC)	53.16	84.99	76.10	79.53	81.78	70.85	71.90
Engineering procurement and construction (EPC)	67.51	107.94	96.65	101.00	103.86	89.98	91.32
Additional costs (AC)	13.29	21.25	19.02	19.88	20.45	17.71	17.98
Installation cost (IC)	80.80	129.18	115.67	120.88	124.31	107.69	109.29
Project contingency (PC)	16.16	25.84	23.13	24.18	24.86	21.54	21.86
Total plant cost (TPC)	96.96	155.02	138.80	145.06	149.17	129.23	131.15
Owner's cost (OC)	14.54	23.25	20.82	21.76	22.38	19.39	19.67
CAPEX	111.50	178.27	159.63	166.82	171.55	148.62	150.82

economic performance of the BHP process using different solvents was compared with that of ECSB process. Table 15 shows the CAPEX of the SMR process without and with a carbon capture process. The economic

performance of BHP with different solvents and configurations are evaluated. The CAPEX of the standard SMR process with the capacity of 200 $t_{\rm H2}/day$ is \$111.5 million. The integration of PCC process with 30

Table 16

The economic performance of commercial-scale BHP process with different configurations.

	SMR without carbon capture	BHP with 30 wt.% MEA	BHP with 30 wt. % PZ	BHP with 38 wt. % PZ	BHP with 44 wt. % PZ	ECSB with 30 wt. % PZ	ECSB with 38 wt. % PZ
CAPEX (Million \$)	111.50	178.27	159.63	166.82	171.55	148.62	150.82
ACC (Million \$/yr)	12.28	19.64	17.59	18.38	18.90	16.37	16.62
Fixed O&M costs (Million \$/yr)	7.55	3.99	2.86	3.24	3.51	2.15	2.23
Variable O&M costs (Million \$/yr)	53.60	88.92	82.10	86.54	96.82	71.81	73.20
TAC (Million \$/yr)	73.43	112.55	102.55	108.16	119.23	90.34	92.04
LCH (\$/t _{H2})	1125.15	1724.62	1571.32	1657.35	1826.97	1384.28	1410.32
CAC (\$/t _{CO2})	N/A	55.67	40.92	47.49	62.12	29.00	31.34

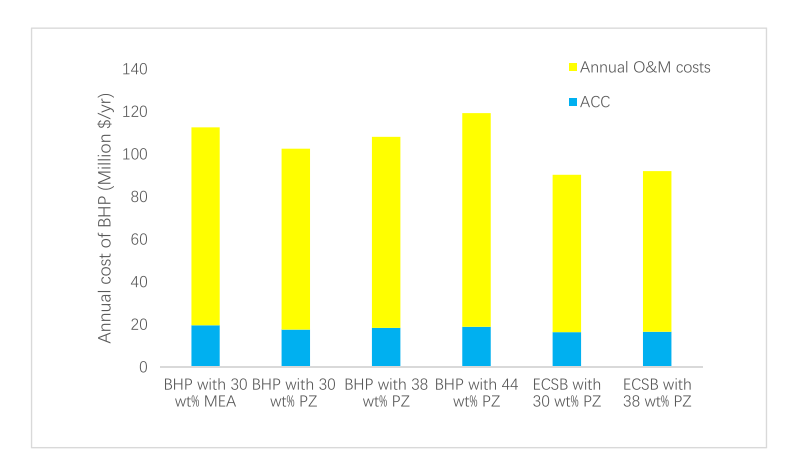


Fig. 10. TAC of commercial-scale BHP using different solvents and configurations.

wt.% MEA significantly increases the CAPEX by 59.9 %. Compared to the BHP process with 30 wt.% MEA, the use of 30-44 wt.% PZ reduces the CAPEX by 3.8 %-10.5 %. This is because PZ has a higher CO2 absorption capacity than MEA, so PZ can achieve 90 % CO₂ capture with a lower solvent circulation rate. This results in smaller absorbers and strippers being required. The ECSB process further reduces the CAPEX by around 16 %, which achieved by the DEC reduction in the stripper. This configuration adopted AFS to replace the standard stripper. In the standard stripper the hot CO₂ vapour is cooled by a condenser at the top of the column while the CO₂-rich solvent is heated by a reboiler at the bottom of the column. In AFS, the wasted exergy in the hot CO₂ vapour is recovered to heat the cold rich bypass. Thus, a smaller sized condenser is required by AFS compared to the standard stripper. Also, the wasted exergy in flue gas is recovered to heat the CO₂ rich solvent. Therefore, a small steam heater is required to instead of the standard reboiler. This results in a reduction in cost of 33.8 % for stripper.

The TAC, levelized cost of H₂ (LCH) and CO₂ avoidance cost (CAC) are shown in Table 16. The TAC of the standard SMR process without carbon capture is \$73.43 million/yr, while the LCH is around 1126 \$/tH2. These results are consistent with current cost of producing hydrogen from natural gas (1000–3000 \$/tH2) (Massarweh et al., 2023). The economic performance of 44 wt.% PZ is unsatisfactory, as it results in the highest values for TAC, levelized cost of blue hydrogen (LCBH) and CAC. Although, the energy performance of 44 wt.% PZ is better than that of 30 wt.% MEA, the variable O&M costs of 44 wt.% PZ is slightly higher than that of 30 wt.% MEA. In simulation, we found that the high PZ loss at high concentration is the main reason for the variable O&M increase. The LCBH and CAC of BHP process with 30 wt.% MEA are 1725 $\frak{1}{4}\frak{1}{4}$ and 56 $\frak{1}{4}\frak{1}{4}\frak{1}{4}$. These results closely align with the findings of Khan et al. (Khan et al., 2021) and Roussanaly et al. (Roussanaly et al., 2020). Khan et al. simulated a SMR plant with a capacity of 200 t/H2 integrated with a PCC plant using MEA. The LCH was estimated to be between 1411 and 1917 \$/tH2. Meanwhile, Roussanaly et al. simulated a SMR plant

with a capacity of 450 $t/_{H2}$ integrated with a PCC plant using MEA. The LCH and CAC were estimated at 1884 t_{H2} and 67 t_{CO2} . The lowest LCBH of around 1389 t_{H2} and lowest CAC of around 33 t_{H2} are achieved by the ECSB process with 30 wt.% PZ. Compared to the BHP process with 30 wt.% MEA, the LCBH and CAC are reduced by 19.7 % and 47.9 % respectively.

Fig. 10 shows the TAC of commercial-scale BHP with different solvents and configurations. It can be seen that the main contribution to the changes of TAC is the variation in the annual O&M costs. The use of 30 wt.% PZ solvents and energy and cost-saving configuration in BHP has clear advantages in reducing TAC, which resulting in the reduction of LCBH and CAC.

4. Conclusions

With the highly increase of global hydrogen demand, the deployment of commercial-scale BHP is becoming important for reducing carbon emission from hydrogen production. The technical and economic performance of BHP was investigated through modelling and simulation. In this study, steady-state models for an SMR process and PCC process were developed in Aspen plus® V11. The SMR process was validated at commercial scale with data from the IEA. The PCC model was validated at pilot scale with experimental data from the literature and then scaled up to process the flue gas from the SMR plant.

Technical analysis was performed to evaluate the energy performance of commercial-scale BHP process. The results showed that the highest energy penalty of 59.32 % was obtained in BHP with 30 wt.% MEA. The least total energy consumption of 213 MW was achieved by ECSB with 30 wt.% PZ. Compared with BHP with 30 wt.% MEA, it reduced the energy penalty by 36.35 %.

The economic analysis was performed in APEA. The results showed that the CAPEX and TAC of the SMR process without carbon capture are \$111.5 million and \$73.4 million/yr respectively. The highest CAPEX

increase of 60 % and TAC increase of 53 % were achieved by BHP process with 30 wt.% MEA. The least CAPEX increase of 33 % and TAC increase of 23 % were achieved by ECSB process with 30 wt.% PZ.

As the first detailed study on TEA of commercial-scale BHP process, this paper provided insights into the energy and cost requirements associated with this process. These findings hold significance for policymakers contemplating the commercial-scale implementation of BHP.

CRediT authorship contribution statement

Yiming Li: Conceptualization, Data curation, Methodology, Software, Validation, Writing – original draft. Jiayi Ren: Conceptualization, Methodology, Software. Haotian Ma: Conceptualization, Methodology, Software. Alasdair N Campbell: Supervision, Writing – review & editing.

Declaration of competing interest

The authors declare that they have no known competing financial interests or personal relationships that could have appeared to influence the work reported in this paper.

Data availability

Data will be made available on request.

Acknowledgement

This research did not receive any specific grant from funding agencies in the public, commercial, or not-for-profit sectors.

Supplementary materials

Supplementary material associated with this article can be found, in the online version, at doi:10.1016/j.ijggc.2024.104112.

References

- Strategy, H., 2020. Enabling a low-carbon economy. Energy.
- Zhongming Z, Linong L, Xiaona Y, Wangqiang Z, Wei L. 2019 Refinement to the 2006 IPCC guidelines for national greenhouse gas inventories. 2019.
- IEA. Hydrogen, IEA, Paris. https://www.iea.org/reports/hydrogen. 2021.
- Faheem, HH, Tanveer, HU, Abbas, SZ, Maqbool, F., 2021. Comparative study of conventional steam-methane-reforming (SMR) and auto-thermal-reforming (ATR) with their hybrid sorption enhanced (SE-SMR & SE-ATR) and environmentally benign process models for the hydrogen production. Fuel 297, 120769.
- Soltani, R, Rosen, M, Dincer, I., 2014. Assessment of CO2 capture options from various points in steam methane reforming for hydrogen production. Int. J. Hydrogen. Energy 39 (35), 20266–20275.
- Khan, MHA, Daiyan, R, Neal, P, Haque, N, MacGill, I, Amal, R, 2021. A framework for assessing economics of blue hydrogen production from steam methane reforming using carbon capture storage & utilisation. Int. J. Hydrogen. Energy 46 (44), 22685–22706.
- Howarth, RW, Jacobson, MZ., 2021. How green is blue hydrogen? Energy Sci. Eng. 9 (10), 1676–1687.
- de Fátima Palhares, DDA, Vieira, LGM, Damasceno, JJR, 2018. Hydrogen production by a low-cost electrolyzer developed through the combination of alkaline water electrolysis and solar energy use. Int. J. Hydrogen. Energy 43 (9), 4265–4275.
- Collodi G, Azzaro G, Ferrari N, Santos S, Brown J, Cotton B, et al. Techno-economic evaluation of SMR based standalone (merchant) hydrogen plant with CCS. IT Report, Editor. 2017.
- Power, G, Busse, A, MacMurray, J., 2018. Demonstration of Carbon Capture and Sequestration of Steam Methane Reforming Process Gas Used For Large-Scale Hydrogen Production. Air Products and Chemicals, Inc., Allentown, PA (United States).
- IEAGHG summary report of the shell quest carbon capture and storage project. In: Preston, C (Ed.), 2018. 14th Greenhouse Gas Control Technologies Conference Melbourne.
- Terrien, P, Lockwood, F, Granados, L, Morel, T., 2014. CO2 capture from H2 plants: implementation for EOR. Energy Procedia 63, 7861–7866.
- Antonini, C, Pérez-Calvo, J-F, Van Der Spek, M, Mazzotti, M., 2021. Optimal design of an MDEA CO2 capture plant for low-carbon hydrogen production—A rigorous process optimization approach. Sep. Purif. Technol. 279, 119715.

- Papalas, T, Antzaras, AN, Lemonidou, AA., 2020. Intensified steam methane reforming coupled with Ca-Ni looping in a dual fluidized bed reactor system: a conceptual design. Chem. Eng. J. 382, 122993.
- Pellegrini, LA, De Guido, G, Moioli, S., 2020. Design of the CO2 removal section for PSA tail gas treatment in a hydrogen production plant. Front. Energy Res. 8, 77.
- Roussanaly S, Anantharaman R, Fu C. Low-carbon footprint hydrogen production from natural gas: a techno-economic analysis of carbon capture and storage from steammethane reforming. 2020.
- Capocelli, M, Luberti, M, Inno, S, D'Antonio, F, Di Natale, F, Lancia, A, 2019. Post-combustion CO2 capture by RVPSA in a large-scale steam reforming plant. J. CO2 Utilizat. 32. 53–65.
- Subraveti, SG, Roussanaly, S, Anantharaman, R, Riboldi, L, Rajendran, A., 2021. Technoeconomic assessment of optimised vacuum swing adsorption for post-combustion CO2 capture from steam-methane reformer flue gas. Sep. Purif. Technol. 256, 117832.
- Otitoju, O, Oko, E, Wang, M., 2021. Technical and economic performance assessment of post-combustion carbon capture using piperazine for large scale natural gas combined cycle power plants through process simulation. Appl. Energy 292, 116893.
- Mandal, B, Bandyopadhyay, S., 2005. Simultaneous absorption of carbon dioxide and hydrogen sulfide into aqueous blends of 2-amino-2-methyl-1-propanol and diethanolamine. Chem. Eng. Sci. 60 (22), 6438–6451.
- Zhang, X, Zhang, C-F, Liu, Y., 2002. Kinetics of absorption of CO2 into aqueous solution of MDEA blended with DEA. Ind. Eng. Chem. Res. 41 (5), 1135–1141.
- Rayer, AV, Sumon, KZ, Sema, T, Henni, A, Idem, RO, Tontiwachwuthikul, P., 2012. Part 5c: solvent chemistry: solubility of CO2 in reactive solvents for post-combustion CO2. Carbon. Manage 3 (5), 467–484.
- Rinker, EB, Ashour, SS, Sandall, OC., 1996. Kinetics and modeling of carbon dioxide absorption into aqueous solutions of diethanolamine. Ind. Eng. Chem. Res. 35 (4), 1107–1114.
- Edali, M, Aboudheir, A, Idem, R., 2009. Kinetics of carbon dioxide absorption into mixed aqueous solutions of MDEA and MEA using a laminar jet apparatus and a numerically solved 2D absorption rate/kinetics model. Internat. J. Greenhouse Gas Control 3 (5), 550–560.
- Derks, P, Kleingeld, T, Van Aken, C, Hogendoorn, J, Versteeg, G., 2006. Kinetics of absorption of carbon dioxide in aqueous piperazine solutions. Chem. Eng. Sci. 61 (20), 6837–6854.
- Liang, ZH, Rongwong, W, Liu, H, Fu, K, Gao, H, Cao, F, et al., 2015. Recent progress and new developments in post-combustion carbon-capture technology with amine based solvents. Internat. J. Greenhouse Gas Control 40, 26–54.
- Van Wagener, DH, Rochelle, GT, Chen, E., 2013. Modeling of pilot stripper results for CO2 capture by aqueous piperazine. Internat. J. Greenhouse Gas Control 12, 280–287.
- Plaza, JM, Rochelle, GT., 2011. Modeling pilot plant results for CO2 capture by aqueous piperazine. Energy Procedia 4, 1593-1600.
- Gao, T, Selinger, JL, Rochelle, GT., 2019. Demonstration of 99 % CO2 removal from coal flue gas by amine scrubbing. Internat. J. Greenhouse Gas Control 83, 236–244.
- Diego, ME, Bellas, J-M, Pourkashanian, M., 2018. Techno-economic analysis of a hybrid CO2 capture system for natural gas combined cycles with selective exhaust gas recirculation. Appl. Energy 215, 778–791.
- Rezazadeh, F, Gale, WF, Rochelle, GT, Sachde, D., 2017. Effectiveness of absorber intercooling for CO2 absorption from natural gas fired flue gases using monoethanolamine solvent. International J. Greenhouse Gas Control 58, 246–255.
- Li, K, Cousins, A, Yu, H, Feron, P, Tade, M, Luo, W, et al., 2016. Systematic study of aqueous monoethanolamine-based CO2 capture process: model development and process improvement. Energy Sci. Eng. 4 (1), 23–39.
- Dilmac, OF, Ozkan, SK., 2008. Energy and exergy analyses of a steam reforming process for hydrogen production. International J. Exergy 5 (2), 241–248.
- Chen, B, Liao, Z, Wang, J, Yu, H, Yang, Y., 2012. Exergy analysis and CO2 emission evaluation for steam methane reforming. Int. J. Hydrogen. Energy 37 (4), 3191–3200
- Simpson, AP, Lutz, AE., 2007. Exergy analysis of hydrogen production via steam methane reforming. Int. J. Hydrogen. Energy 32 (18), 4811–4820.
- Ermatchkov, V, Á, Pérez-Salado Kamps, Speyer, D, Maurer, G, 2006. Solubility of carbon dioxide in aqueous solutions of piperazine in the low gas loading region. J. Chemical Eng. Data 51 (5), 1788–1796.
- Canepa, R, Wang, M, Biliyok, C, Satta, A., 2013. Thermodynamic analysis of combined cycle gas turbine power plant with post-combustion CO2 capture and exhaust gas recirculation. J. Process Mech. Eng. 227 (2), 89–105.
- Posey, ML, Rochelle, GT., 1997. A thermodynamic model of Methyldiethanolamine—CO2—H2S—Water. Ind. Eng. Chem. Res. 36 (9), 3944–3953.
- Hetzer, HB, Robinson, R, Bates, RG., 1968. Dissociation constants of piperazinium ion and related thermodynamic quantities from 0 to 50. deg. J. Phys. Chem. 72 (6), 2081–2086.
- Ermatchkov, V, Kamps, ÁP-S, Maurer, G., 2003. Chemical equilibrium constants for the formation of carbamates in (carbon dioxide+ piperazine+ water) from 1H-NMRspectroscopy. J Chem Thermodyn 35 (8), 1277–1289.
- Pinsent, B, Pearson, L, Roughton, F., 1956. The kinetics of combination of carbon dioxide with hydroxide ions. Transact. Faraday Soc. 52, 1512–1520.
- Bishnoi, S, Rochelle, GT., 2000. Absorption of carbon dioxide into aqueous piperazine: reaction kinetics, mass transfer and solubility. Chem. Eng. Sci. 55 (22), 5531–5543. Bird, R, Stewart, W, Lightfoot, E., 2007. Transport Phenomena, 2nd Edn. John Wilwe &
- Sons. Inc, New York, NY. Horvath, AL., 1985. Handbook of Aqueous Electrolyte Solutions. Halsted Press.
- Wilke, C, Chang, P., 1955. Correlation of diffusion coefficients in dilute solutions. AIChE journal 1 (2), 264–270.

- Plus, A., 2008. Rate Based model of the CO2 Capture Process By MEA Using Aspen Plus. Aspen Technology Inc, Cambridge, MA, USA.
- Bravo, JL, Rocha, JA, Fair, J., 1985. Mass transfer in gauze packings. Hydrocarbon processing (International ed) 64 (1), 91–95.
- Chilton, TH, Colburn, AP., 1934. Mass transfer (absorption) coefficients prediction from data on heat transfer and fluid friction. IndustrialEng.Chem. 26 (11), 1183–1187.
- Bravo, JL, Patwardhan, AA, Edgar, TF., 1992. Influence of effective interfacial areas in the operation and control of packed distillation columns. Ind. Eng. Chem. Res. 31 (2), 604–608.
- Van Wagener DH. Stripper modeling for CO_2 removal using monoethanolamine and piperazine solvents 2011.
- Agbonghae, E, Hughes, K, Ingham, D, Ma, L, Pourkashanian, M., 2014. Optimal process design of commercial-scale amine-based CO2 capture plants. Ind. Eng. Chem. Res. 53 (38), 14815–14829.
- Sinnott, R., 2005. Chemical engineering design: chemical engineering Volume 6. Elsevier.
- Luo, X., 2016. Process modelling, simulation and optimisation of natural gas combined cycle power plant integrated with carbon capture, compression and transport. University of Hull.

- Lepaumier, H, da Silva, EF, Einbu, A, Grimstvedt, A, Knudsen, JN, Zahlsen, K, et al., 2011. Comparison of MEA degradation in pilot-scale with lab-scale experiments. Energy Procedia 4, 1652–1659.
- Manzolini, G, Fernandez, ES, Rezvani, S, Macchi, E, Goetheer, E, Vlugt, T., 2015.
 Economic assessment of novel amine based CO2 capture technologies integrated in power plants based on European Benchmarking Task Force methodology. Appl. Energy 138, 546–558.
- TRADING ECONOMICS: US natural gas price https://tradingeconomics.com/commo dity/natural-gas [February 2023].
- Karimi, M, Hillestad, M, Svendsen, HF., 2011. Capital costs and energy considerations of different alternative stripper configurations for post combustion CO2 capture. Chem. Engineering Res. Design 89 (8), 1229–1236.
- Gaspar, J, von Solms, N, Thomsen, K, Fosbøl, PL., 2016. Multivariable optimization of the piperazine CO2 post-combustion process. Energy Procedia 86, 229–238.
- Massarwel, O, Al-khuzaei, M, Al-Shafi, M, Bicer, Y, Abushaikha, AS, 2023. Blue hydrogen production from natural gas reservoirs: a review of application and feasibility. J. CO2 Utilizat. 70, 102438.